ELSEVIER

Journal of Alloys and Compounds 408–412 (2006) 1368–1372

Journal of ALLOYS AND COMPOUNDS

www.elsevier.com/locate/jallcom

Fabrication of $SmFe_{12}$/α-Fe thin films as anisotropic nanocomposite magnet

H. Kato [a,*], H. Kubota [a,1], K. Koyama [b], T. Miyazaki [a]

[a] *Department of Applied Physics, Tohoku University, Aoba-yama 6-6-05, 980-8579 Sendai, Japan*
[b] *Institute for Materials Research, Tohoku University, Katahira 2-1-1, 980-8577 Sendai, Japan*

Available online 2 June 2005

Abstract

A series of nanocomposite thin films, composed of α-Fe and *c*-axis oriented $SmFe_{12}$ phases, has been synthesized by rf magnetron sputtering onto heated glass substrates. The volume fraction of α-Fe, V_{Fe}, in the obtained films ranges from 5% to 85%. According to the Rietveld analysis of X-ray diffraction patterns, the *c*-axis of each $SmFe_{12}$ grain was estimated to locate within a cone with its symmetry axis being normal to the film plane and with the cone angle of 7°. For samples with $V_{Fe} < 30\%$, the demagnetization curves with fields applied normal to the film plane have exhibited a good squareness. In small V_{Fe} films, the coercivity H_c increased with increasing V_{Fe}, took a maximum for $V_{Fe} \sim 25\%$, and then decreased. In the reference system of randomly aligned $SmFe_{12}$/α-Fe films, on the other hand, we confirmed that H_c decreased monotonically with increasing V_{Fe}.

Keywords: Magnetic films and multilayers; Nanostructures; Permanent magnets; Exchange and superexchange

1. Introduction

Recent advances in small-scale magnetic devices stimulate the needs of high performance permanent magnet films. Not much work [1–4] so far, however, was done in the field of thin-film rare earth magnet, as compared with the extensive research works on bulk rare earth magnets. Several sputtered $R_2Fe_{14}B$ film (R: rare earth) systems [5–8] have been studied, some of which [6–8] reported a preferred *c*-axis orientation. Cadieu et al. [1] have reported that it is possible, by using rf sputtering, to synthesize binary $SmFe_{12}$ films of the $ThMn_{12}$ structure without third element. This report, thus, demonstrates the advantage of thin-film form, because the bulk $SmFe_{12}$ cannot stabilize the $ThMn_{12}$ structure without adding a third element [9], such as Ti, V, or Mo.

On the other hand, a study of film-type exchange-coupled hard/soft magnets has recently been the one of the main subjects in this field, since the report by Kneller and Hawig [10] and Skomski and Coey [11]. Shindo et al. [12,13] have succeeded in fabricating $Nd_2Fe_{14}B$/α-Fe multilayers. However, the reported values of the maximum energy product $(BH)_{max}$ are much smaller than those for the ideal system [11], since it is not easy to realize ideal nanostructures, such as grain size, its distribution, and alignment of the hard-phase crystallite. Fullerton et al. [14] fabricated the epitaxial SmCo/Fe bilayers as an ideal anisotropic nanocomposite system. However, the obtained value of $(BH)_{max}$ is not so high, since the magnetization of the Sm–Co phase is relatively small.

In the present study, we synthesized the thin-film nanocomposite magnets, composed of α-Fe and *c*-axis oriented $SmFe_{12}$ phases by using rf magnetron sputtering onto heated glass substrates. The hard $SmFe_{12}$ and soft α-Fe phases are placed not in multilayer geometry, but are randomly dispersed in the films. We have chosen this geometry since the coercivity could be larger than that in the multilayer geometry owing to the larger interface area of hard and soft phases in the randomly dispersed geometry. In order to investigate the effect of hard phase alignment on the magnetic properties,

* Corresponding author. Tel.: +81 22 217 7948; fax: +81 22 217 7947.
E-mail address: kato@mlab.apph.tohoku.ac.jp (H. Kato).
[1] Present address: Nanoelectronics Research Institute, AIST, 1-1-1 Umezono, Tsukuba 305-8568, Japan.

0925-8388/$ – see front matter © 2005 Elsevier B.V. All rights reserved.
doi:10.1016/j.jallcom.2005.04.108

we have also synthesized the randomly oriented $SmFe_{12}$/α-Fe nanocomposite films by post-annealing procedure.

2. Experimental

The $SmFe_{12}$/α-Fe nanocomposite films were deposited by rf magnetron sputtering onto glass substrates (Corning 7059) in an Ar atmosphere. The base pressure of the sputtering system was below 4×10^{-7} Torr and the Ar pressure during the sputtering was 60 mTorr. The volume fraction of the α-Fe, V_{Fe}, was adjusted systematically by putting a different number of Sm tips (5 mm × 5 mm) on the disk shaped Fe target with 76 mm diameter. The substrate temperature T_s during the sputtering was fixed to 550 °C after the optimization experiments [15]. To obtain a randomly oriented $SmFe_{12}$, the substrates were not heated during the sputtering and then the films were annealed at 627 °C for 1 h. The films have the forms of glass/Ti (50 nm)/Sm–Fe (1 μm)/Ti (50 nm) or glass/Sm–Fe (1 μm)/Ti (50 nm). The chemical composition was checked by EPMA and EDS attached SEM. The film structure was studied by X-ray diffraction with Cu Kα radiation. Magnetization curves were measured by two kinds of vibrating sample magnetometer systems, with the maximum applied fields of 16 kOe and 140 kOe, respectively. When the field is applied perpendicular to the film plane, a demagnetizing field correction was made by using the coefficient of 4π. The final values of V_{Fe} in the deposited films were estimated by combining the results of Rietveld analysis [16] of X-ray diffraction patterns and the temperature dependence of magnetization at high temperatures.

3. Results and discussion

Typical X-ray diffraction patterns for $SmFe_{12}$/α-Fe films with different values of V_{Fe} are shown in Fig. 1. Although, with increasing V_{Fe}, the intensity of α-Fe peak grows, the intensity of (0 0 2) peak for $SmFe_{12}$ phase keeps the large value up to $V_{Fe} = 48\%$, exhibiting the conservation of the (0 0 1) texture. We then estimated the average grain size of both phases by using the full-width at half maximum (FWHM) data of diffraction peaks and Scherrer's formula, which are plotted against V_{Fe} in Fig. 2a. The average size of α-Fe grain increases with V_{Fe} for $V_{Fe} < 40\%$ and become roughly constant having about 30 nm for $V_{Fe} > 40\%$. In the case of $SmFe_{12}$ grain, estimated values do not depend on V_{Fe} very much and fall into the range of 30–40 nm. In order to obtain an information about the degree of alignment, we made a Rietveld analysis [16] for these patterns, in which easy-axis directions of $SmFe_{12}$ phase are assumed to be distributed according to the March–Dollase function [17] $P(\alpha) = (r^2 \cos^2\alpha + r^{-1} \sin^2\alpha)^{-3/2}$, where α is the angle between the preferred-orientation direction and the normal of a diffraction plane, and r is a parameter representing a degree of alignment. In the case of a perfect alignment $r = 0$,

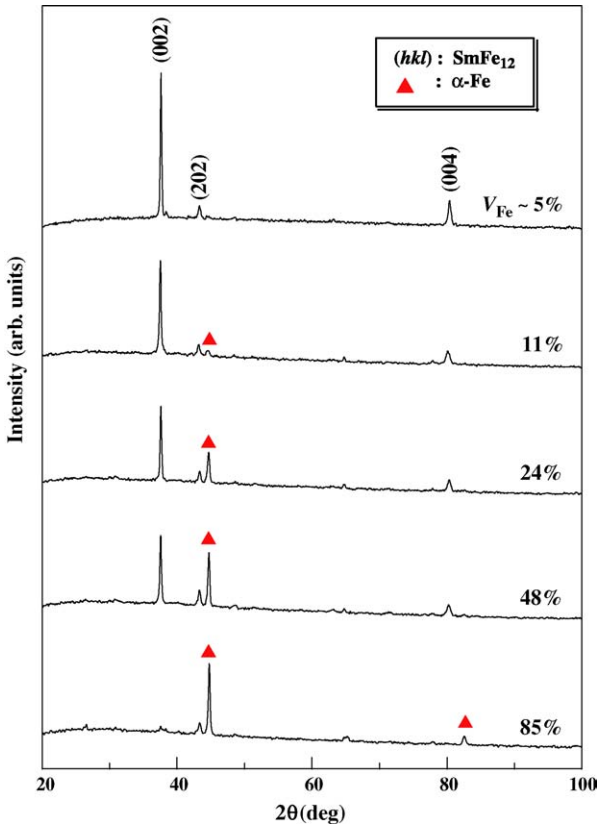

Fig. 1. X-ray diffraction patterns for glass/Sm–Fe/Ti films with different values of α-Fe volume fraction V_{Fe}.

while $r = 1$ for a random alignment. Fig. 2b shows the estimated r parameter for the $SmFe_{12}$ phase as a function of V_{Fe}. We have found that the r value is about 0.3 for $V_{Fe} < 50\%$, which means that half width of distribution of c-axis directions, $\Delta\theta$, is about 7° along the normal of the film plane. This value of $\Delta\theta$ is less than half of that for $Nd_2Fe_{12}B$/α-Fe

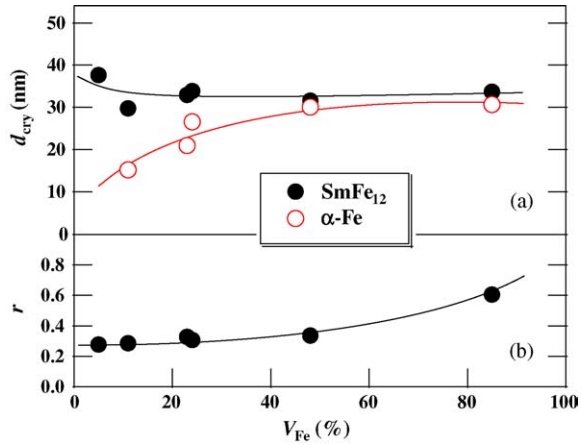

Fig. 2. (a) Average grain size d_{cry} for $SmFe_{12}$ and α-Fe phases deduced from the FWHM of diffraction peaks, plotted against V_{Fe}. (b) Alignment parameter r for the $SmFe_{12}$ phase. Solid lines are guides to the eye.

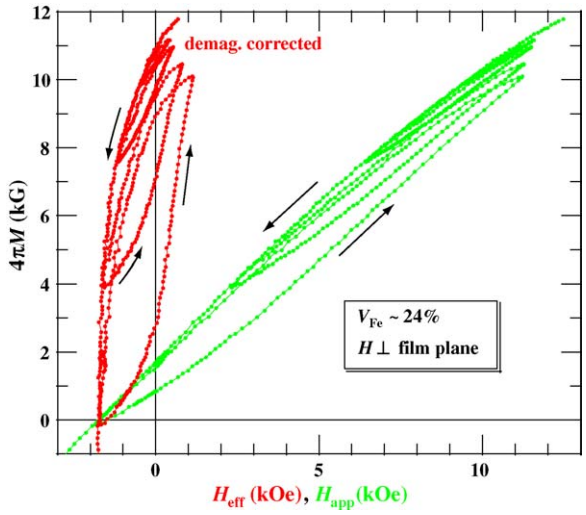

Fig. 3. Magnetization recoil curves for the sample with $V_{Fe} = 24\%$ plotted against both applied field H_{app} and demagnetizing-field-corrected field H_{eff}.

anisotropic nanocomposite films [18], which we fabricated recently.

In Fig. 3, we plotted the magnetization recoil curves for the sample with $V_{Fe} = 24\%$, as a function of both applied field H_{app} and demagnetizing-field-corrected effective field H_{eff}. It is seen that the recoil permeability is quite high, suggesting the occurrence of a spring-back behavior of α-Fe moments owing to the exchange coupling between soft and hard phases.

Major hysteresis loops for a series of films given in Fig. 1 are shown in Fig. 4. For films with $V_{Fe} < 30\%$, demagnetization curves along the easy-axis keep the nice squareness and the hard-axis curves exhibit low magnetization values. It should be noted that, for the larger V_{Fe} films, difference of magnetization curves between parallel and perpendicular directions becomes small and the H_c is also reduced. In order to inspect the variation in magnetic properties with V_{Fe}, the values of saturation magnetization M_s, remanent magnetization M_r, coercive field H_c, and $(BH)_{max}$ are plotted against V_{Fe} in Fig. 5. The value of M_s increases linearly with V_{Fe} within the error bar except for the $V_{Fe} = 48\%$ film, while H_c slightly increases with V_{Fe} and takes a maximum at $V_{Fe} \sim 25\%$, and then decreases for larger V_{Fe}. Reflecting the good squareness of demagnetization curves, M_r keeps large values for $V_{Fe} < 30\%$, which then decreases for higher V_{Fe}. Such a decrease in M_r will possibly be related to the larger size of α-Fe grain for $V_{Fe} > 30\%$ (see Fig. 2a), which causes a magnetization reversal in a center portion of the α-Fe grains. The $(BH)_{max}$ also takes a maximum at $V_{Fe} \sim 25\%$ with the value of 20 MGOe (160 kJ/m^3) and then decreases rapidly, the variation of which can then be interpreted as the combined effect of V_{Fe} dependence of H_c, M_r, M_s, and the squareness. According to the EPMA analysis, Sm content of the $V_{Fe} = 48\%$ film is anomalously larger than the expected value taking account of the volume fraction of α-Fe and $SmFe_{12}$ phases. The

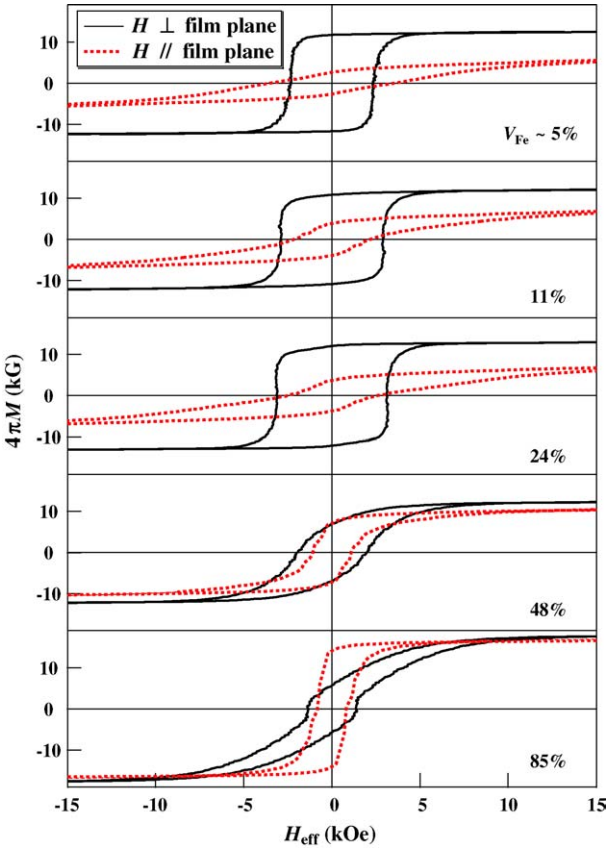

Fig. 4. Magnetization curves for glass/Sm–Fe/Ti films for which X-ray data were shown in Fig. 1. Magnetic fields of up to 140 kOe were applied parallel (dotted curves) and perpendicular (solid curves) to the film plane.

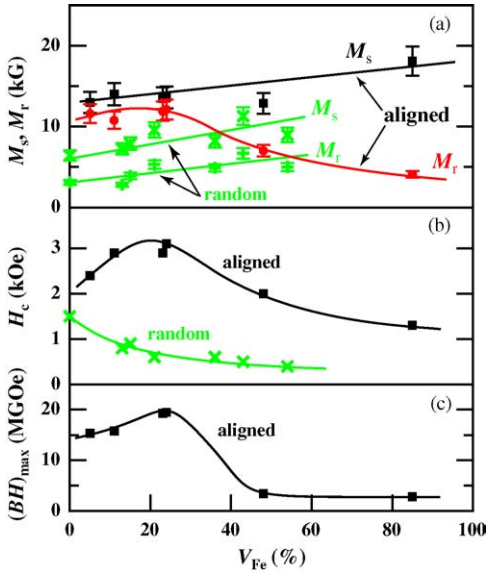

Fig. 5. (a) Saturation magnetization M_s and remanent magnetization M_r, (b) coercive field H_c, and (c) maximum energy product $(BH)_{max}$, as a function of V_{Fe} for aligned and randomly oriented $SmFe_{12}$/α-Fe films.

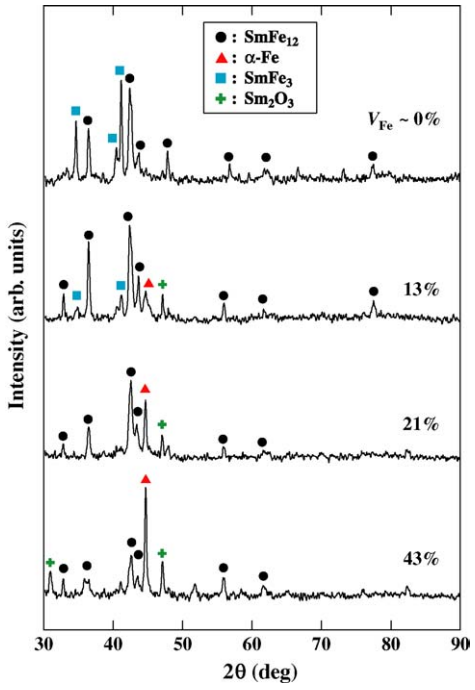

Fig. 6. X-ray diffraction patterns for randomly oriented $SmFe_{12}$/α-Fe films with different volume fractions of the α-Fe phase.

lower M_s value in this film will thus be attributed to the existence of excess Sm, being in the oxide states and/or taking amorphous forms.

Since none of previous works on the nanocomposite magnets reported the H_c increase with increasing fraction of soft magnetic phase, present maximum behavior of H_c seems to be a unique feature of the aligned hard-phase system. To confirm this conjecture, we have fabricated a series of randomly oriented $SmFe_{12}$/α-Fe nanocomposite films by using the rf magnetron sputtering onto non-heated substrates and the subsequent annealing. X-ray diffraction patterns of the obtained films are shown in Fig. 6, which exhibit reflections of the crystalline phases for $SmFe_{12}$, α-Fe, and small amount of $SmFe_3$ and Sm_2O_3. The relative intensity of the α-Fe peak is seen to increase with V_{Fe}. After measuring the magnetization curves, the dependence of M_s, M_r, and H_c on V_{Fe} is plotted in Fig. 5, together with those for aligned $SmFe_{12}$/α-Fe films. The H_c value does decrease monotonically with V_{Fe}, which is in contrast with the present aligned system, but in agreement with the calculated H_c for random system [19]. In a partially aligned hard/soft nanocomposite system such as the present film, H_c is expected to be strongly dependent on both the degree of hard phase alignment [20] and the magnitude of exchange coupling J between the grains [21]. The J value would depend on the interfacial state of grain boundary [22]. Sun et al. [3] reported that, by the TEM observation of their $SmFe_{12}$ films, the cubic $SmFe_2$ phase were found to exist in the grain-boundary region of the main $SmFe_{12}$ phase. Existence of such a $SmFe_2$ phase in the present films with small V_{Fe} was also confirmed by the temperature dependence of magnetization. We thus speculate that the H_c increase phenomena observed here would be related to the enhancement of J owing to the reduction of volume-fraction of such a grain boundary phase.

4. Conclusion

A series of $SmFe_{12}$/α-Fe nanocomposite films with different values of V_{Fe} has been synthesized by rf magnetron sputtering onto heated substrates. The crystallite of $SmFe_{12}$ was confirmed to be aligned so that the c-axis of $ThMn_{12}$ structure is perpendicular to the film plane. The magnetization curves showed a nice squareness, reflecting the high orientation of the $SmFe_{12}$ easy-axis. With increasing V_{Fe}, M_s increased linearly, while H_c slightly increased and took a maximum at $V_{Fe} \sim 25\%$. The $(BH)_{max}$ value of 20 MGOe was obtained for $V_{Fe} = 25\%$ film. This value is still too small to compare with the ideally estimated one [11] or the one for more realistic situation [20]. Further investigations are necessary especially to find an optimum condition to reduce the volume fraction of grain boundary phases, which will then enhance both M_s and H_c, and hence $(BH)_{max}$.

Acknowledgements

We are grateful to Takuya Nomura and Masahiko Ishizone for their cooperation. This work was partly supported by the Iketani Science and Technology Foundation.

References

[1] F.J. Cadieu, H. Hegde, A. Navarathna, R. Rani, K. Chen, Appl. Phys. Lett. 59 (1991) 875.
[2] D. Wang, S.H. Liou, P. He, D.J. Sellmyer, G.C. Hadjipanayis, Y. Zang, J. Magn. Magn. Mater. 124 (1993) 62.
[3] H. Sun, T. Tomida, S. Hirosawa, J. Appl. Phys. 81 (1997) 328.
[4] E.E. Fullerton, J.S. Jiang, C.H. Sowers, J.E. Pearson, S.D. Bader, Appl. Phys. Lett. 72 (1998) 380.
[5] F.J. Cadieu, T.D. Cheung, L. Wickramasekara, J. Magn. Magn. Mater. 54–57 (1986) 535.
[6] J.F. Zasadzinski, C.U. Serge, E.D. Rippert, J. Appl. Phys. 61 (1987) 4278.
[7] S. Yamashita, J. Yamazaki, M. Ikeda, N. Iwabuchi, J. Appl. Phys. 70 (1991) 6627.
[8] K.D. Aylesworth, D.J. Sellmyer, G.C. Hadjipanayis, J. Magn. Magn. Mater. 98 (1991) 65.
[9] K. Ohashi, T. Yokoyama, R. Osugi, Y. Tawara, IEEE Trans. Magn. MAG-23 (1987) 3101.
[10] E.F. Kneller, R. Hawig, IEEE Trans. Magn. 27 (1991) 3588.
[11] R. Skomski, J.M.D. Coey, Phys. Rev. B 48 (1993) 15 812.
[12] M. Shindo, M. Ishizone, H. Kato, T. Miyazaki, A. Sakuma, J. Magn. Magn. Mater. 161 (1996) L1.
[13] M. Shindo, M. Ishizone, A. Sakuma, H. Kato, T. Miyazaki, J. Appl. Phys. 81 (1997) 4444.
[14] E.E. Fullerton, J.S. Jiang, M. Grimsditch, C.H. Sowers, S.D. Bader, Phys. Rev. B 58 (1998) 12 193.

[15] H. Kato, T. Nomura, M. Ishizone, H. Kubota, T. Miyazaki, J. Appl. Phys. 87 (2000) 6125.
[16] F. Izumi, T. Ikeda, Mater. Sci. Forum 321-324 (2000) 198.
[17] W.A. Dollase, J. Appl. Crystallogr. 19 (1986) 267.
[18] H. Kato, M. Ishizone, K. Koyama, T. Miyazaki, J. Magn. Magn. Mater. 290–291 (2005) 1221.
[19] R. Fischer, T. Schrefl, H. Kronmüller, J. Fidler, J. Magn. Magn. Mater. 150 (1995) 329.
[20] H. Fukunaga, H. Nakamura, IEEE Trans. Magn. 36 (2000) 3285.
[21] R. Fischer, H. Kronmüller, Phys. Rev. B 54 (1996) 7284.
[22] H. Kato, M. Ishizone, T. Miyazaki, K. Koyama, H. Nojiri, M. Motokawa, IEEE Trans. Magn. 37 (2001) 2567.